Archives of Biochemistry and Biophysics xxx (2011) xxx–xxx

Contents lists available at SciVerse ScienceDirect

Archives of Biochemistry and Biophysics

journal homepage: www.elsevier.com/locate/yabbi

Mutation of Phe413 to Tyr in catalase KatE from *Escherichia coli* leads to side chain damage and main chain cleavage ☆

Vikash Jha, Lynda J. Donald, Peter C. Loewen *

Department of Microbiology, University of Manitoba, Winnipeg, Canada MB R3T 2N2

ARTICLE INFO

Article history:
Available online xxxx

Keywords:
Catalase
KatE
Main chain cleavage
Side chain modification

ABSTRACT

The monofunctional catalase KatE of *Esherichia coli* exhibits exceptional resistance to heat denaturation and proteolytic degradation. During an investigation of subtle conformation changes in Arg111 and Phe413 on the proximal side of the heme induced by H_2O_2, variants at position R111, T115 and F413 were constructed. Because the residues are not situated in the distal side heme cavity where catalysis occurs, significant changes in reactivity were not expected and indeed, only small changes in the kinetic characteristics were observed in all of the variants. However, the F413Y variant was found to have undergone main chain cleavage whereas the R111A, T115A, F413E and F413K variants had not. Two sites of cleavage were identified in the crystal structure and by mass spectrometry at residues 111 and 115. In addition to main chain cleavage, modifications to the side chains of Tyr413, Thr115 and Arg111 were suggested by differences in the electron density maps compared to maps of the native and inactive variant H128N/F413Y. The inactive variant H128N/F413Y and the active variant T115A/F413Y both did not exhibit main chain cleavage and the R11A/F413Y variant exhibited less cleavage. In addition, the apparent modification of three side chains was largely absent in these variants. It is also significant that all three F413 single variants contained heme b suggesting that the fidelity of the phenyl group was important for mediating heme b oxidation to heme d. The reactions are attributed to the introduction of a new reactive center possibly involving a transient radical on Tyr413 formed during catalytic turn over.

Introduction

Catalases are found in virtually all aerobic organisms speaking to the underlying importance of the enzyme's protective role in removing H_2O_2 ($2H_2O_2 \rightarrow 2H_2O + O_2$) before it or its breakdown products cause cellular damage. Generally, the absence of catalatic activity does not have a striking effect on growth, but does affect long term survival in an aerobic or oxidative environment [1].

Escherichia coli produces one monofunctional catalase, KatE or HPII (hydroperoxidase II)[1] [2,3], and one catalase-peroxidase, KatG or HPI [4]. While KatG is produced in response to oxidative stress during logarithmic phase growth [3], KatE is produced only in stationary phase as part of the RpoS regulon [5]. It is a large subunit clade 2 enzyme [6] that has a relatively slow turnover rate compared to some small subunit catalases [7], but exhibits unusual resistance to temperature, proteolysis and high H_2O_2 concentrations [7–10].

KatE has been the object of a long term structure function study that has provided extensive insights into the catalatic reaction and identified several unusual structural features unique to KatE. As part of these studies, over 100 variants of the enzyme have been constructed and characterized. Among these were H128N and H128A where removal of the essential histidine in the distal side heme pocket produced an inactive enzyme [11]. These variants were used to identify potential binding sites for H_2O_2 in the entrance channel and heme cavity [12]. Curiously, H_2O_2 caused a change in the conformation of Phe413 in two of the subunits, C and D but not in A and B, whereas the nearby Arg111 underwent a conformational change in subunits A and B, but not in C and D [12]. The proximity of Phe413 in subunits A and B and Arg111 in subunits C and D and their relation to the two fold symmetry axis and heme centers is shown in Fig. 1.

The asymmetry of these conformation changes, their proximity to the heme, its proximal ligand Tyr415 and nearby His392, all of which undergo post-translational modification in the presence of substrate H_2O_2, suggested a possible functional significance to the changes. A site-directed mutagenesis and structural study of a series of variants of Phe413 and the neighboring Arg111 and Thr115 was undertaken to investigate this possibility. Unexpect-

☆ The coordinates for the structures included in this manuscript have been submitted with PDB accession codes 3TTT (F413Y), 3TTU (F413Y/H128N), 3TTV (F413Y/T115A), 3TTW (F413E), and 3TTX (F413K).

* Corresponding author. Fax: +1 204 474 7603.
E-mail addresses: ploewen@ms.umanitoba.ca, peter_loewen@umanitoba.ca (P.C. Loewen).

[1] *Abbreviations used:* HPII, hyperperoxidase II; WT, wild type; TAFY, T115A/F413Y; FY, F413Y; FE, F413E.

0003-9861/$ - see front matter © 2011 Published by Elsevier Inc.
doi:10.1016/j.abb.2011.11.022

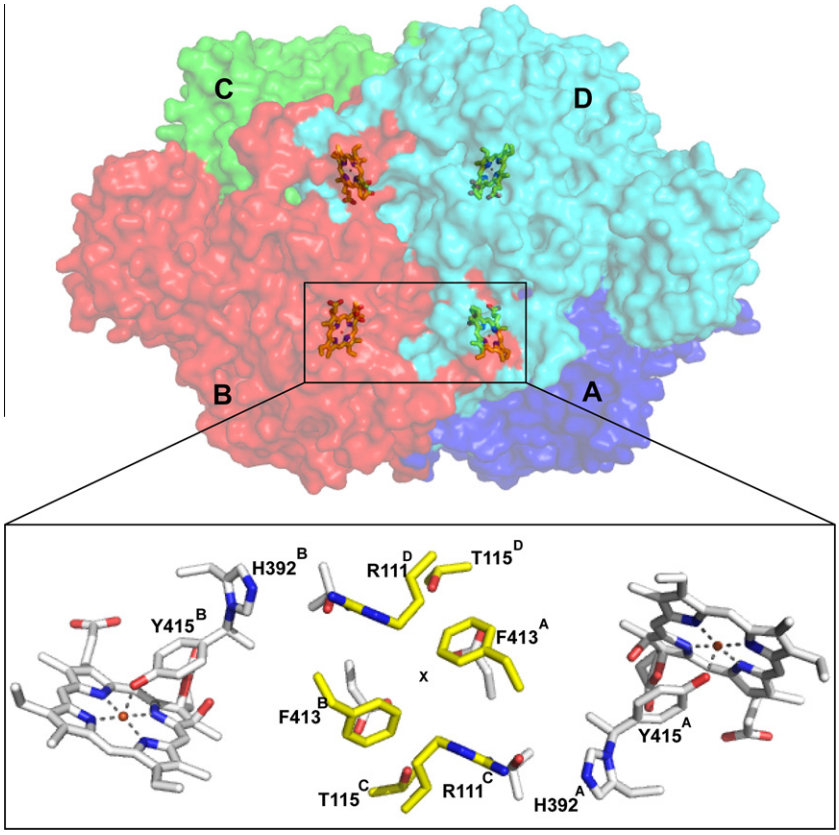

Fig. 1. Organization of residues Arg111, Thr115 and Phe413 on the proximal sides of the heme in KatE. In panel A, the tetrameric structure of HPII is shown with the subunits distinguished by color and letter: A in blue, B in red, C in green and D in cyan. The hemes in the four subunits are shown and those from subunits A and B are boxed. This section is rotated slightly to generate the view in panel B where the relationship of Arg111 and Thr115 in subunits C and D to Phe413 ahd heme in subunits A and B is shown. The covalent junction between Tyr415 and His392 is also shown. The location of the two fold axis of symmetry is indicated by the X.

edly, it was found that replacement of Phe with Tyr introduced a new reactive center into the protein which led to side chain modification and strand cleavage.

Material and methods

Variant protein construction, purification and characterization

Standard chemicals and biochemicals were obtained from Sigma. The oligonucleotides GGACGTTTGGCCTCCTATACC (F413A), GGACGTTTGGAGTCCTATACC (F413E), GGACGTTTGCAGTCCTATACC (F413Q), GGACGTTTGAAATCCTATACC (F413K), GGACGTTTGTACT CCTATACC(F413Y), TTTATTCTGGCCGAGAAAATC (R111A), TTTATT CTGAAAGAGAAAATC (R111K) and GAGAAAATCGCCCACTTTGAC (T115A) were purchased from Invitrogen and used to mutate the *Eco*RI–*Cla*I fragment (base pairs 1856–3466) or the *Pst*I–*Hind*III fragment (base pairs 1–1246) of pAMkatE72 [13] following the Kunkel procedure [14] as previously described [15]. The mutated sequences were confirmed [16] and used to generate the plasmids pF413A, pF413E, pF413Q, pF413K, pF413Y, pR111A, pR111K and pT115A by reincorporating the fragment into the full length katE gene. The plasmids pH128N and pH392N had been constructed previously. The native and variant proteins were expressed and purified as described [15]. Catalase activity was determined by the method of Rørth and Jensen [17] in a 1.8 mL reaction volume using a Gilson oxygraph equipped with a Clark electrode. One unit of catalase is defined as the amount that decomposes 1 mol of H_2O_2 in 1 min in a 60 mM H_2O_2 solution at pH 7.0 and 37 °C. The initial rates of oxygen evolution were used to determine the turnover rates (Table 1) to minimize inactivation caused by a high concentration of H_2O_2. Protein was estimated according to the methods outlined by Layne [18]. All spectra were obtained using a Milton Roy MR3000 spectrophotometer.

Mass spectrometry

Slices from SDS–PAGE gels were treated as described [19] after which digested samples were mixed with an equal volume of matrix (2,5-dihydroxybenzoic acid) and deposited on a metal plate that fits into a MALDI QqTOF mass spectrometer [20]. Spectra were acquired and analyzed using software developed in the time-of-flight laboratory in the Department of Physics and Astronomy. Output data with 20 ppm error and up to 1 missed cleavage site were submitted online to MASCOT at www.matrixscience.com. All possible ions from peptides of the N-terminus from both wild type and the F413Y variant were selected for tandem mass spectra; those data were analysed by visual comparison of the ions expected from the known sequence to those observed in the spectrum.

Crystallization and structure determination

Crystals of the HPII variants were obtained at 22 °C using the hanging drop vapor diffusion method over a reservoir solution containing 15–17% PEG 3350 (Carbowax), 1.6–1.7 M LiCl and 0.1 M Tris pH 9.0 [21,22]. The crystals were monoclinic, space group $P2_1$ with one tetrameric molecule in the crystal asymmetric unit. Data sets were collected using synchrotron beam line CMCF 08ID-1 at the Canadian Light Source in Saskatoon, Canada from crystals flash cooled in the reservoir buffer. Diffraction data were processed and scaled using programs MOSFLM and SCALA [23], respectively (Table 2). To determine if any structural changes were being caused by X-ray irradiation, three blocks of 90 images from

Table 1
Kinetic comparison of the F413, R111 and R115 variants of KatE.

Variant	Specific activity (units/mg)	k_{cat} (s^{-1})	K_M (app) (mM)	k_{cat}/K_M ($M^{-1}\,s^{-1}$)
Native	21,000 ± 1400	70,000	145	4.8×10^5
F413A	16,000 ± 160	24,200	56	4.3×10^5
F413E	16,800 ± 640	69,800	200	3.5×10^5
F413K	13,400 ± 160	85,560	196	4.4×10^5
F413Q	11,300 ± 280	57,700	120	4.8×10^5
F413Y	16,000 ± 1400	81,640	160	5.1×10^5
R111A	19,500 ± 1000	80,000	140	5.7×10^5
R111A/F413Y	15,000 ± 500	76,270	440	1.7×10^5
T115A	22,070 ± 530	191,510	718	2.7×10^5
T115A/F413Y	16,900 ± 1260	151,835	460	3.3×10^5
H128N/F413Y	Not detectable	–	–	–
H392Q/F413Y	8400 ± 280	69,840	590	1.2×10^5

three different crystals were merged into single data sets using SCALA. Structure refinement starting with native KatE structure (1GGE) was completed using program REFMAC [24] and manual modeling with the molecular graphics program COOT [25]. The Ramachandran distribution of residues for all structures was ~96%, 3.5% and 0.5%, respectively in favored, allowed and outlier regions. Figures were generated using PYMOL (The PYMOL Molecular Graphics System, Schrödinger, LLC).

Results

Construction and kinetic characterization of F413 variants

Residues Arg111 and Phe413 in *E. coli* catalase KatE are situated on the heme proximal side about 12 Å from the heme iron and either 5.5 or 8.5 Å, respectively, from both the Nδ of His392 that is linked to Cβ of Tyr415 as part of a post-translational process [26]. To investigate the response of Phe413 and Arg111 to added H_2O_2, they were mutated to a variety of residues that introduced acidic, basic, uncharged polar, and aliphatic side chains. Specifically, plasmids harboring mutated *katE* genes encoding R111A, R111K, F413A, F413E, F413Q, F413K and F413Y were constructed. All variants accumulated normal amounts of protein confirming that protein folding was not affected by the mutations.

The kinetic parameters of the variants reveal slightly reduced catalatic specific activity and near normal turnover rates and apparent K_M values with the exception of F413A and T115A, with respectively lower and higher turnover rates than the native enzyme (Table 1 and Fig. 2A). The term "apparent K_M" in the context of catalases is H_2O_2 concentration at 1/2 V_{max} and is used because the catalatic reaction does not strictly saturate with substrate and therefore does not precisely follow Michaelis–Menten kinetics [7]. Whereas small subunit catalases are typically inhibited by concentrations of H_2O_2 above 300–500 mM at which point there is no further increase in velocity, large subunit catalases like HPII are much more resistant to inhibition by high concentrations of H_2O_2. This is illustrated by up to 5 M H_2O_2 being employed in the assays to reach maximum velocity (Fig. 2A). The oxygraph assay makes the employ of such extreme concentrations possible, circumventing the need for extrapolation and its inherent uncertainties.

A comparison of the absorbance spectra of WT HPII and its F413Y variant reveals significant differences in the charge transfer bands (Fig. 2B) with the WT enzyme having a predominant band at 590 nm typical of heme d and F413Y having a series of weaker bands including one at 630 nm typical of heme b. Preparations of WT HPII always contain small amounts (5–10%) of heme b, probably a result of incomplete conversion [11], consistent with the small shoulder peak at 630 nm (Fig. 2B). F413Y does exhibit a small

Table 2
Data collection and refinement statistics.

A – Data collection statistics					
Variant	F413Y	F413Y/H128N	F413Y/T115A	F413E	F413 K
PDB	3TTT	3TTU	3TTV	3TTW	3TTX
Unit cell parameters					
a (Å)	93.56	93.62	93.56	93.49	93.50
b (Å)	133.33	132.96	133.05	133.85	132.96
c (Å)	122.16	122.67	122.64	122.68	122.03
α, γ (°)	90.0	90.0	90.0	90.0	90.0
β (°)	109.58	109.39	109.29	109.36	109.69
Resolution[a]	29.4–1.58 (1.67–1.58)	41.4–1.89 (2.0–1.89)	34.2–1.45 (1.53–1.45)	31.3–1.62 (1.71–1.62)	35.2–1.74 (1.83–1.74)
Unique reflections	376939 (54792)	189038 (21370)	483215 (66864)	311384 (46552)	278274 (37423)
Completeness%	98.9 (98.6)	84.3 (65.5)	96.9 (92.0)	87.1 (89.3)	97.2 (89.8)
R_{merge}	0.121 (0.564)	0.062 (0.214)	0.085 (0.492)	0.085 (0.581)	0.106 (0.458)
$\langle I/\sigma I \rangle$	7.3 (2.3)	14.9 (5.1)	7.9 (2.1)	9.2 (2.0)	9.7 (2.9)
Multiplicity	4.3 (4.1)	3.9 (3.6)	3.4 (3.2)	3.6 (3.4)	3.7 (3.3)
B – Model refinement statistics					
No. reflections	357889	179396	458621	295502	264164
R_{cryst} (%)	15.7	14.4	14.5	15.6	14.6
R_{free} (%)	18.9	19.3	17.2	19.9	18.5
Non-H atoms	26185	25998	26534	26013	26025
Water molecules	3008	2840	3361	2835	2856
Average B-factor Å²					
Protein	15.4	15.2	14.9	16.3	13.3
Heme	8.3	8.5	9.0	11.3	7.9
Waters	26.1	21.4	25.9	25.5	21.5
Other					
Coor. err. Å[b]	0.056	0.081	0.037	0.059	0.063
Rms dev. bonds Å	0.024	0.022	0.027	0.022	0.022
Rms dev. angles (°)	2.02	1.98	2.66	1.98	1.98

[a] Values in parentheses correspond to the highest resolution shell.
[b] Based on maximum likelihood.

Please cite this article in press as: V. Jha et al., Arch. Biochem. Biophys. (2011), doi:10.1016/j.abb.2011.11.022

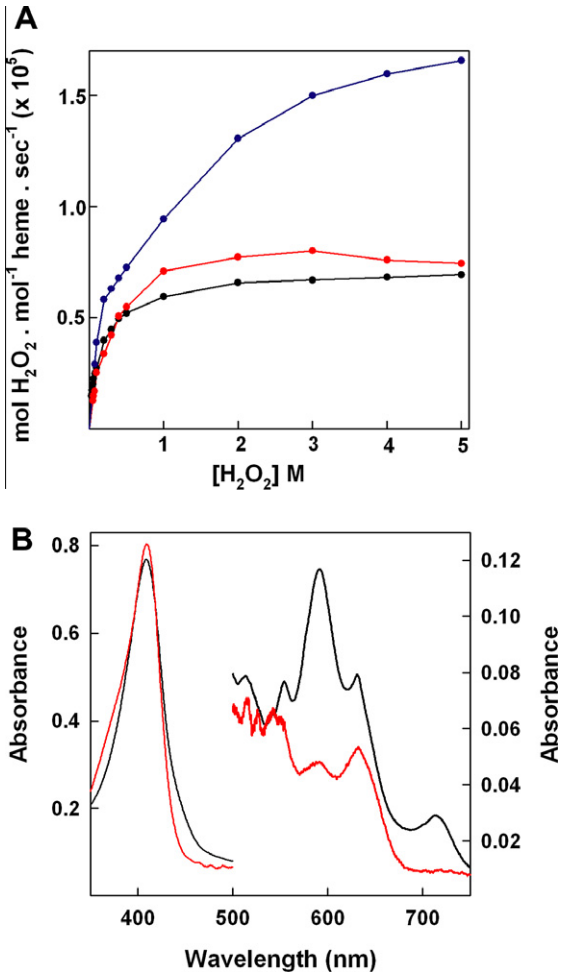

Fig. 2. Kinetic and spectral features of HPII and selected variants. In panel A, the relationship of velocity to H_2O_2 concentration is shown for the native enzyme (black), F413Y (red) and T115A (blue). A summary of the kinetic constants from these and related data is contained in Table 1. In panel B, the absorbance spectra of native HPII (black) and F413Y (red) are shown. The scale on the right applies to the range 500–750 nm.

peak at 590 nm that may suggest a small amount of heme d, but, as will be described below, there is too little to be distinguished in the electron density maps calculated for structure refinement. In summary, changes to Phe413 had little effect on catalytic efficiency, but did seem to interfere with post-translational heme modification.

Apparent proteolysis in F413Y

In light of the minimal influence on catalysis of the F413Y mutation, it was surprising to find the variant subunit to be predominantly 74 kDa with only a small amount of the expected 84 kDa band (Fig. 3). This suggested a proteolytic event unique to F413Y, but the addition of the common protease inhibitors PMSF and EDTA to the purification solutions did not reduce the amount of chain breakage. In addition, the extreme resistance to protease cleavage exhibited by KatE [9] made it unlikely that a protease would act so uniquely on just one variant. Significantly, there was no evident protein cleavage in the inactive double variant H128N/F413Y, which lacks the essential distal His. Despite this apparent link between cleavage and catalytic activity, attempts to demonstrate protein cleavage of the 84 kDa band in vitro by treatment variously with H_2O_2, ascorbate, glucose/glucose oxidase

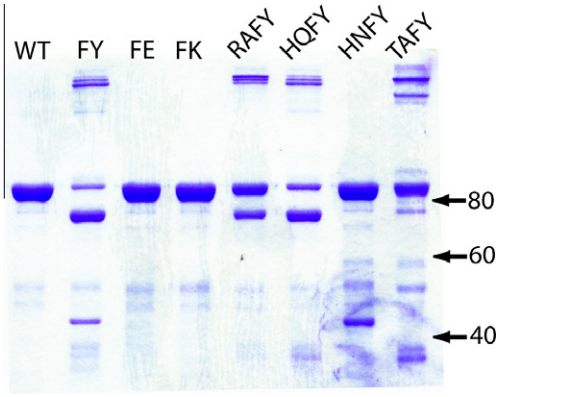

Fig. 3. SDS polyacrylamide electrophoresis analysis of KatE variants constructed for this study. The location of size markers (kDa) is indicated by the arrows. The lanes are WT, wild type; FY, F413Y; FE, F413E; FK, F413K; RAFY, R111A/F413Y; HQFY, H392Q/F413Y; HNFY, H128N/F413Y; TAFY, T115A/F413Y.

or xanthine/xanthine oxidase for up to 24 h at room temperature were not successful.

To identify the site of chain cleavage whether closer to the N- or C-terminus, the 74 kDa protein band of cleaved F413Y variant and the 84 kDa protein band of wild type HPII were subjected to MALDI MS analysis following trypsin digestion. A comparison of the two sets of trypsin fragments identified a number of bands that were absent in the shorter variant protein. These were identified by MS–MS analysis as being residues 88–96, 101–111 and 114–121, whereas the 131–142 peptide was present in both spectra (Fig. 4A and B). The intervening two peptides 122–125 and 126–130 were too small to be identified, but it was clear that protein cleavage had occurred prior to residue 131 consistent with the loss of approximately 10 kDa.

Structural characterization of the F413 variants

To provide a more precise structural definition of the region around F413 in the variant, their structures were determined by X-ray crystallography. Crystals of F413E, F413K and F413Y were prepared and used to collect X-ray diffraction data that refined to between 1.9 and 1.5 Å (Table 2). The electron density maps define the main chain and side chain atoms of 2904 amino acids, four heme groups and 3200–3500 waters in four subunits. As in the native structure, the N-terminal 27 residues are not visible, but for F413E and F413K, the maps show complete continuity from Ser28 to Ala753 in all four subunits. The expected side chains of glutamate and lysine at position 413 are evident for each although the replacement side chains exhibited greater mobility than the original phenyl group (*B* values > 30 $Å^2$). In addition the side chains of the nearby Arg111 and Gln419 occupy new or partially new conformations, the latter because of its interaction with the heme propionate when not oxidized to heme d.

In contrast to the other F413 variants where the replacement side chains were well defined in the electron density, there was almost no electron density that could be assigned to the Tyr413 side chain of F413Y. This could be interpreted as being a result of disorder, but the maps of the same region in the inactive double variant F413Y/H128N clearly showed the tyrosine side chain to be present (Fig. 5A and B) suggesting that the side chain was largely missing in F413Y. The apparent loss of the Tyr413 side chain was correlated with three other structural changes in the immediate vicinity which were evident in the F_o–F_c omit maps calculated with the model absent. The first is the apparent partial loss or increased disorder of the R111 side chain (Fig. 4C and D); the second is the partial loss or modification of Thr115 (Fig. 4C and D); and the third

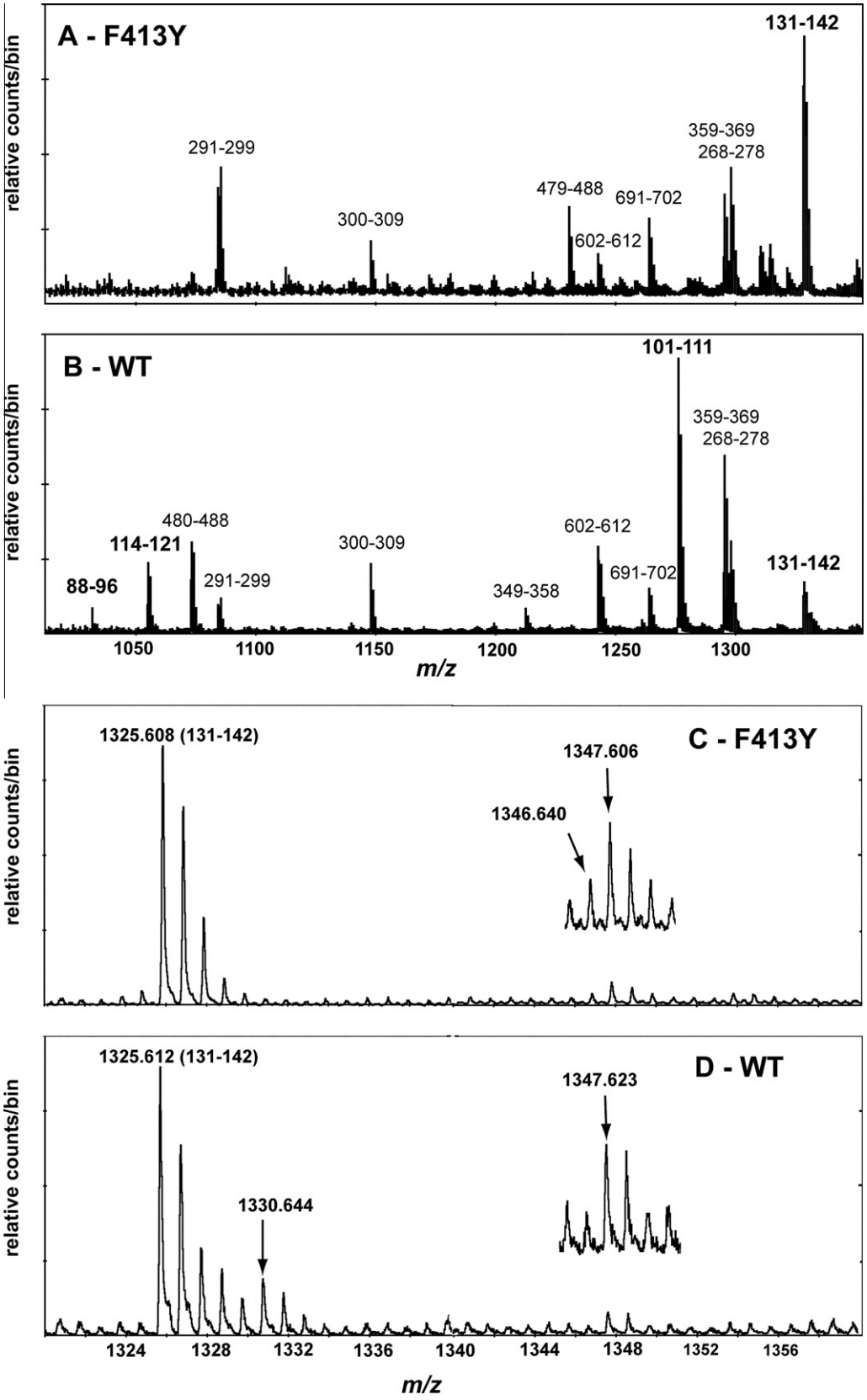

Fig. 4. MALDI spectra of tryptic digests of the 74 kDa band of the F413Y variant and the 84 kDa WT enzyme. In panel A (F413Y) and panel B (WT), the ions in the mass range *m/z* 1000–1350 Da are labeled with their sequence identity and the ions in bold were confirmed by MS–MS analysis. The conclusion from panels A and B is that there are no ions matching the first 130 amino acids in F413Y. In panels C (F413Y) and D (WT), the *m/z* from 1300 to 1360 is enlarged to focus on the peptide containing residue 413 (LY^{413}SYTDTQISR (1346 Da) in panel C and LF^{413}SYTDTQISR (1330 Da) in panel D). The 1330 ion is clearly evident in panel D and its sequence was confirmed by MS–MS analysis. The 1346 ion in panel C is evident only in the inset with a 5× enlargement of the *y* axis. Attempts to carry out MS–MS analysis on the small amount of 1346 ion to confirm its identity were unsuccessful. The small amount of 1347 ion in both spectra was not identified but serves as a useful standard.

Please cite this article in press as: V. Jha et al., Arch. Biochem. Biophys. (2011), doi:10.1016/j.abb.2011.11.022

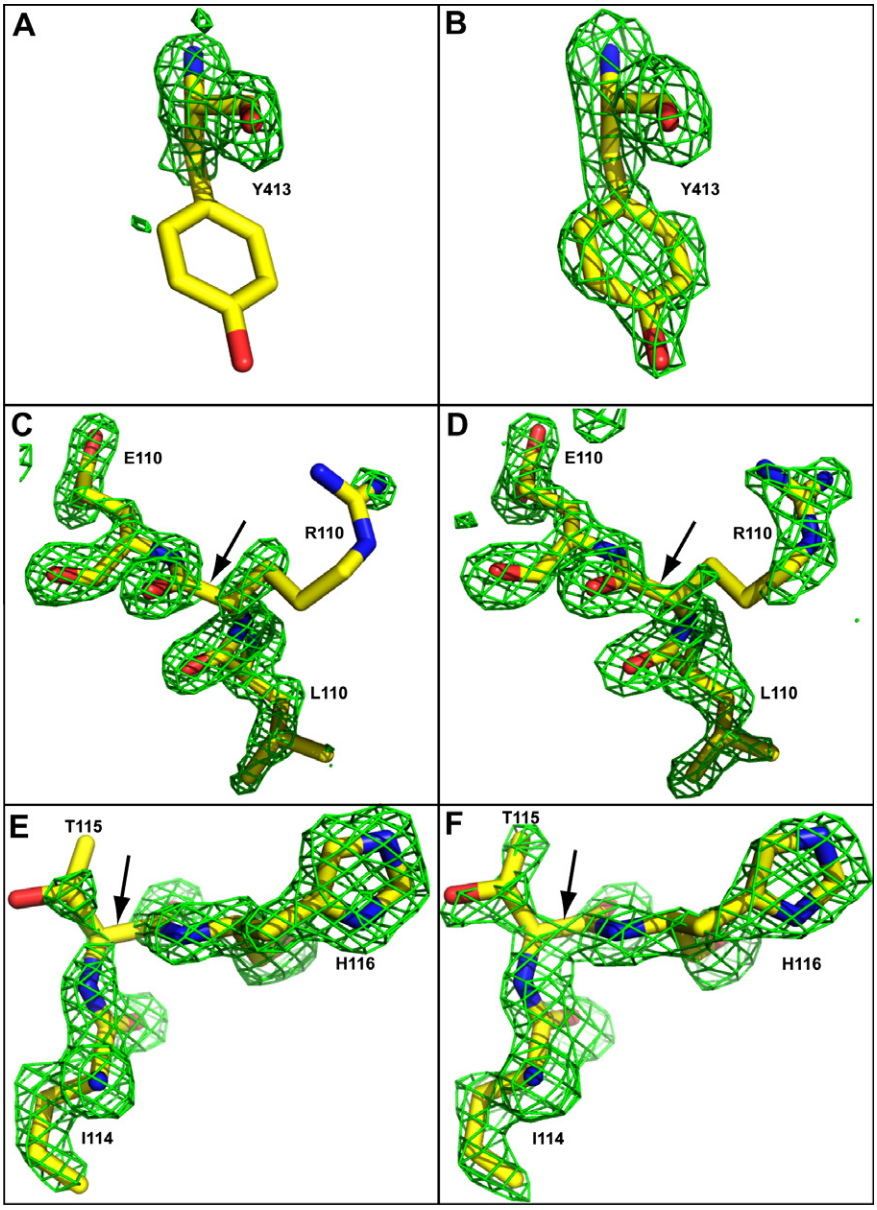

Fig. 5. Electron density maps corresponding to regions of Tyr413 variant without (panels A, C and E) and with the H128N mutation also present (panels B, D and F). Tyr413 which is evident in panel B is absent in panel A. In panels C and D, residues 110–112 are shown with the arrows indicating the region of main chain electron density that is absent in C but present in D. Note also the much weaker density corresponding to R111 in panel C. In panels E and F, residues 114–116 are which with the arrows indicating the region of main chain density that is absent in E but present in F. Note also the much weaker density corresponding to T115 in panel E. The F_o–F_c electron density maps, drawn in green at $\sigma = 3.0$ (3.5 in panels C and D), were calculated without the protein segments in the model and the appropriate models are superimposed.

is the apparent cleavage of the main chain at two locations, evident in gaps in the electron density between residues 111 and 112 (Fig. 4C and D) and between 115 and 116 (Fig. 4C and D). These putative cleavage sites correlate well with the absence of peptides corresponding to the first 120 residues of the protein. Damage from X-ray irradiation contributing to side chain modification and main chain cleavage was ruled out by the absence of any differences among maps of the region calculated from the merging of images from multiple crystals after short, medium and long exposure times (first 90, middle 90 and last 90 images) (data not shown).

Further support for the loss of the phenol group of Tyr413 was gleaned from a comparison of tryptic peptides from the native enzyme and the F413Y variant. The peptide containing F413 (residues 412–422, LF^{413}SYTDTQISR) has an expected *m/z* of 1330 and an ion pattern centered on 1330 is evident in the spectrum of the native enzyme, albeit partially obscured by overlap with the tail of more abundant ions of the 131–142 envelope centered at 1325, but absent in the F413Y spectrum (Fig. 4C and D). The identity of the 1330 ion was confirmed by MS–MS analysis. The expected 412–422 ion envelope from the F413Y variant containing Y413, centered at 1346, is present in only very small amounts (Fig. 4C) compared to the 1330 ion in the native spectrum (Fig. 4D) and the small amounts led to unsuccessful attempts at sequence confirmation by MS–MS analysis. The apparent low yields of the 1330 ion cluster compared to the 1325 ion cluster prompted an examination of the spectra for partial digest fragments at 2776/2792 and 5092/5108 Da, but none were found. Similarly, an examination of the spectra of F413Y for peptides arising from the degradation of the 1346 ion was unsuccessful, perhaps not surprising in light of the continuum of degradation evident in the electron density maps and the low yields of the 1330 ion. In conclusion, the 412–422 peptide is confirmed in the MS spectrum of the native enzyme, while the small amount of the peptide in the spectrum of

F413Y is consistent with degradation of the peptide in the variant, but precluded sequence verification.

The changes noted in the side chains of Arg111 and Thr115 in combination with their close proximity to Tyr413, involving a short hydrogen bond interaction in the case of Thr115, suggested that they may be involved in the reactive process that removes the tyrosine side chain and cleaves the protein chain. This was confirmed in the case of Thr115 when the T115A/F413Y variant was found to exhibit very little cleavage (Fig. 3) and had an intact Tyr413 side chain. A lesser involvement of the Arg111 was suggested by the reduced but still evident main chain cleavage in the R111A/F413Y variant.

Whereas the turnover rate of F413Y did not change significantly from that of the native enzyme, the absorbance spectrum (Fig. 2B) suggested that the self-catalyzed heme oxidation to heme d had not occurred. The predominance of heme b in the variant was confirmed in the crystal structure where electron density maps (not shown) were consistent with > 90% heme b. By contrast, the nearby His392–Tyr415 covalent link, a post-translational modification, was present in F413Y, although elimination of the His–Tyr bond did not affect protein cleavage or loss of the tyrosine side chain in the His392Q/F413Y variant. Thus, the three post-translational processes on the proximal side of the heme, heme modification, His–Tyr bond formation and the Tyr413 mediated reactions, occur independent of one another despite their close proximity.

Discussion

The minor changes in kinetic properties of the F413 and R111 variants of *E. coli* KatE suggest that the residues do not have a direct role in the catalatic process. They are adjacent to the access channel leading from the central cavity to the proximal side of the heme that presumably provides access for the H_2O_2 involved in His392–Tyr415 cross linking and heme oxidation. Consequently, the cause of the changes in orientation of Arg111 and Phe413 induced by H_2O_2 in the H128N variant may simply be a result of their proximity to un-reacted H_2O_2 in the core of the protein, but this does not explain why the changes occur in only one of the two distal side regions, that with R111 from subunits A and B and F413 from subunits C and D. The second distal side region with R111 from subunits C and D and F413 from subunits A and B (shown in Fig. 1) was not affected. Involvement of the region in the catalytic process is also evident in the enhanced turnover rate of the T115A variant which may suggest an alternate access route to the heme cavity at high substrate concentrations.

The inherent reactivity of the region on the proximal side of the heme in KatE is evident in the rapid oxidation events leading to the His392–Tyr415 linkage and heme d during the first few rounds of catalysis. Introduction of Tyr at position 413 creates a potential radical center facilitated by the ionic environment created by the nearby Arg111 and Asp417. In addition, the phenol of Tyr413 becomes part of a hydrogen bond matrix that includes a water and the side chains of Asp417, Asp118 and Ser414 linking it to the heme (Fig. 6). The short 2.3 Å hydrogen bond of the Tyr413 OH with the OH of Thr115 is particularly noteworthy. It is present in the inactive H128N/F413Y variant and would presumably also stabilize the phenol side chain in F413Y reducing disorder compared to T115A/F413Y where the hydrogen bond is missing. This is inconsistent with the explanation of disorder for the disappearance of the phenol ring in F413Y. On the other hand, the hydrogen bond may be an essential part of the reaction pathway bringing about destruction of the phenol, modification of the threonine side chain and main chain cleavage. The reduced amount of cleavage in R111A/F413Y suggests that the side chain of Arg111 may also have a role in the process. Consistent with heme oxidation to heme d and His–Tyr cross link formation being mutually independent, destruction of the phenol ring of Tyr413 and nearby main chain cleavage occurred independently of these other reactions. The reason for reduced heme d formation in the F413 variants is not clear since the phenyl ring should be relatively unreactive. One possibility is that like the main channel of catalases which are lined with a very high proportion of phenylalanines, Phe413 may maintain the integrity of a channel for movement of H_2O_2 to the proximal side of the heme and heme oxidation.

The extent of the damage including loss of the phenol ring of Tyr413, oxidation of the Thr115 side chain to what resembles

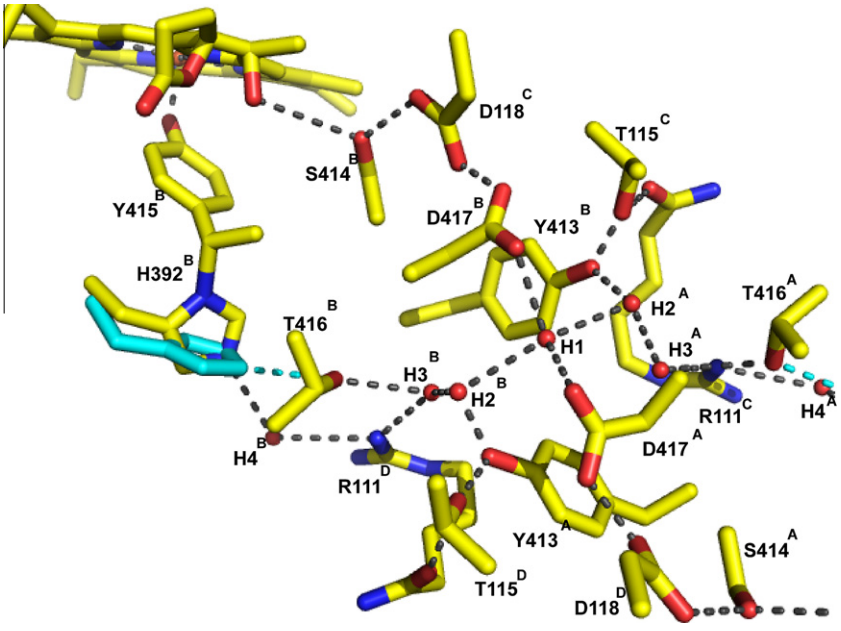

Fig. 6. Hydrogen bond matrix linking the Tyr–His and heme reactive centers with Tyr413. Water H1 is located on the two-fold symmetry axis and the symmetrically located waters progressing towards the hemes in subunits A and B are labeled $H2^A$, $H2^B$, etc. His392 and the H-bond to Thr416 colored cyan are as situated prior to covalent linkage to Try415.

Please cite this article in press as: V. Jha et al., Arch. Biochem. Biophys. (2011), doi:10.1016/j.abb.2011.11.022

CH_3–C═O, the loss or disorder of the Arg111 side chain and the cleavage of the main chain at residues 111 and 115 all caused by placing Tyr at position 413 in KatE is remarkable. KatE has evolved to be highly resistant to protease cleavage [9] and heat treatment [8] and remains active after the removal of 74 N-terminal residues, 189 C-terminal residues and a 20 residue internal fragment [10]. Indeed the inherent protease resistance where even 16 h incubation with proteinase K did not cut the main chain near residues 111 and 115 [10] provides strong corroboration that the main chain cleavage deep within the quaternary structure of the protein is not the result of protease action. However, in light of the previous success in demonstrating heme modification in vitro [11], the inability to demonstrate F413Y main chain cleavage in vitro was perplexing. A definitive explanation is lacking, but one possibility is that reactive species may exist in vivo during growth that facilitate cleavage and we cannot re-create the necessary species by simple H_2O_2 or ascorbate treatment in vitro.

The extensive damage including three modified side chains and main chain cleavage at two nearby locations largely precludes the definition of a comprehensive reaction mechanism. The absence of heme oxidation may be a result of radical formation on Tyr413 supplying an electron to the heme porphyrin radical, thereby interfering with its oxidation to heme d. The Tyr radical then leads to the subsequent reactions, but whether they are concerted or separate is not clear. It is perhaps significant that the phenol rings of Tyr413 in the T115A/F413Y variant are 0.4 Å closer together than the phenyl rings in the native enzyme (3.22 compared to 3.65 Å) providing a greater opportunity for interaction. There is also a direct link between the apparent oxidation of the side chain of Thr115 and the two sites of main chain cleavage. One site is at residue 115 while the second is at Arg111, and the Thr115 OH is hydrogen bonded with the C═O of Arg111 as well as the phenol OH of Tyr413. Unfortunately, there are simply too many unknowns to propose a meaningful mechanism for so many interrelated changes. For example, we do not know if H_2O_2 is directly involved, whether or not electron transfer to or from the heme is involved, whether or not Tyr413 becomes a radical site, why the H-bond to Thr115 is essential or whether or not a reactive species unique to in vivo conditions in involved.

Most commonly among catalases the residue at the equivalent to Phe413 is one of the non-polar Val, Ile, Leu or Phe with Ser or Thr appearing less commonly. Cat-3 of *Neurospora crassa* is currently the only known catalase with a Tyr (residue 387) at the equivalent position [27]. Like KatE, Cat-3 is a large subunit catalase, but its proximal environment appears much less reactive than that of KatE. The His of the proximal His–Tyr linkage of KatE is replaced by a Gln (residue 366) and the heme is unmodified heme b. Furthermore, the environment of Tyr387 in Cat3 does not appear to be as conducive to radical formation being some distance from the nearest Asp (residue 391). In addition, the closest non-solvent contact of the Tyr387 OH is with Gln89 at 3.5 Å, providing little catalytic opportunity for reaction. Notably, the equivalent of Thr115 in HPII is an alanine in Cat3.

Conclusions

The variant F413Y of catalase KatE of *E. coli* contains a new reactive center that leads to loss of the Tyr413 side chain, modification of the nearby Arg111 and Thr115 side chains and main chain cleavage at Thr115 and Arg111. Catalytic turnover and the Thr115 side chain are required for the reactions to occur.

Acknowledgments

This work was supported by a Discovery Grant 9600 from the Natural Sciences and Engineering Research Council of Canada (to P.C.L.), by the Canada Research Chair Program (to P.C.L.). Research described in this paper was performed at the Canadian Light Source, which is supported by the Natural Sciences and Engineering Research Council of Canada, the National Research Council Canada, the Canadian Institutes of Health Research, the Province of Saskatchewan, Western Economic Diversification Canada, and the University of Saskatchewan.

References

[1] P. Nicholls, I. Fita, P.C. Loewen, Advances in Inorganic Chemistry 51 (2001) 51–106.
[2] P.C. Loewen, Journal of Bacteriology 157 (1984) 622–626.
[3] P.C. Loewen, J. Switala, B.L. Triggs-Raine, Archives of Biochemistry and Biophysics 243 (1985) 144–149.
[4] P.C. Loewen, B.L. Triggs-Raine, C.S. George, B.E. Hrabarchuk, Journal of Bacteriology 162 (1985) 661–667.
[5] P.C. Loewen, R. Henge-Aronis, Annual Review of Microbiology 48 (1994) 53–80.
[6] M.G. Klotz, P.C. Loewen, Molecular Biology and Evolution 20 (2003) 1098–1112.
[7] J. Switala, P.C. Loewen, Archives of Biochemistry and Biophysics 401 (2002) 145–154.
[8] J. Switala, J. O'Neil, P.C. Loewen, Biochemistry 38 (1999) 3895–3901.
[9] P. Chelikani, L.J. Donald, H.W. Duckworth, P.C. Loewen, Biochemistry 42 (2003) 5729–5735.
[10] P. Chelikani, X. Carpena, R. Perez-Luque, L.J. Donald, H.W. Duckworth, J. Switala, I. Fita, P.C. Loewen, Biochemistry 44 (2005) 5597–5605.
[11] P.C. Loewen, J. Switala, I. von Ossowski, A. Hillar, A. Christie, B. Tattrie, P. Nicholls, Biochemistry 32 (1993) 10159–10164.
[12] W. Melik-Adamyan, J. Bravo, X. Carpena, J. Switala, M.J. Mate, I. Fita, P.C. Loewen, Proteins 44 (2001) 270–281.
[13] I. von Ossowski, M.R. Mulvey, P.A. Leco, A. Borys, P.C. Loewen, Journal of Bacteriology 173 (2001) 514–520.
[14] T.A. Kunkel, J.D. Roberts, R.A. Zakour, Methods in Enzymology 154 (1987) 367–382.
[15] P. Chelikani, X. Carpena, I. Fita, P.C. Loewen, Journal of Biological Chemistry 278 (2003) 31290–31296.
[16] F.S. Sanger, S. Nicklen, A.R. Coulson, Proceedings of the National Academy of Sciences of the United States of America 74 (1977) 5463–5467.
[17] H.M. Rørth, P.K. Jensen, Biochimica et Biophysica Acta 139 (1967) 171–173.
[18] E. Layne, Methods in Enzymology 3 (1957) 447–454.
[19] A. Shevchenko, H. Tomas, J. Havlis, J.V. Olsen, Nature Protocols 1 (2006) 2856–2860.
[20] A.V. Loboda, A.N. Krutchinsky, M. Bromirski, W. Ens, Rapid Communications in Mass Spectrometry 14 (2000) 1047–1057.
[21] J. Bravo, N. Verdaguer, J. Tormo, C. Betzel, J. Switala, P.C. Loewen, I. Fita, Structure 3 (1995) 491–502.
[22] J. Bravo, M.J. Maté, T. Schneider, J. Switala, K. Wilson, P.C. Loewen, I. Fita, Proteins 34 (1999) 155–166.
[23] Collaborative Computational Project, Number 4, The CCP4 Suite: programs for protein crystallography, Acta Crystallographica D50 (1994) 760–763.
[24] G.N. Murshudov, A.A. Vagin, E.J. Dodson, Acta Crystallographica D53 (1997) 240–255.
[25] P. Emsley, K. Cowtan, Acta Crystallographica D60 (2004) 2126–2132.
[26] J. Bravo, I. Fita, J.C. Ferrer, W. Ens, A. Hillar, J. Switala, P.C. Loewen, Protein Science 6 (1997) 1016–1023.
[27] A. Diaz, V.J. Valdes, E. Rudino-Pinera, R. Arreola, W. Hansberg, Journal of Molecular Biology 386 (2009) 218–232.